Shutter-Speed Model DCE-MRI Detection of Tumor Hypoxia: Initial Experience

Ellen Ackerstaff[1], Xin Li[2], Sohyun Han[3], DongKyu Lee[3], HyungJoon Cho[3], Sean Carlin[1], Jason A Koutcher[1], and Wei Huang[2]

[1]Memorial Sloan-Kettering Cancer Center, New York, NY, United States, [2]Oregon Health & Science University, Portland, OR, United States, [3]Ulsan National Institute of Science and Technology (UNIST), EonYang-eup, Ulju-gun, Ulsan, Korea, Republic of

Background/Objective: The non-invasive detection and quantification of hypoxic areas in tumors has been of tremendous interest, since hypoxic cancer cells are more resistant to treatment and thus, tumor hypoxia has been related to treatment outcome and patient survival[2-4]. Hypoxia imaging and the identification of tumor necrosis early after the start of treatment facilitate the assessment of treatment response before tumor shrinkage occurs[3]. Clinically and preclinically, dynamic contrast enhanced ^{1}H MRI (DCE-MRI) has been used to characterize the leaky and chaotic vasculature in tumors[5-8]. Recently, Cho *et al.* imaged the tumor microenvironment in a preclinical tumor model, using *in vivo* DCE-MRI plus ^{18}F-Fmiso PET and *ex vivo* immunohistochemical and histological validation[1]. The tumor Ak_{ep} value, a measure of tumor perfusion/permeability derived from DCE-MRI data analysis using the Hoffmann model[9], was able to distinguish well-perfused from necrotic tumor tissue, while the *in vivo* identification of hypoxic areas required the additional acquisition of ^{18}F-Fmiso PET. The Shutter-Speed model[7, 8] (SSM) for DCE-MRI pharmacokinetic data analysis accounts for finite inter-compartmental water exchange effects. In addition to the conventional K^{trans} and v_e parameters, the SSM analysis also returns a third parameter, the mean intracellular water molecule lifetime τ_i. A recent yeast cell suspension study shows that τ_i is inversely correlated to cell membrane ion ATPase kinetics, a measure of metabolic activity[10]. *Using the experimental DCE-MRI data obtained by Cho et al.[1], we investigate whether DCE-MRI biomarkers obtained from SSM analysis can separate perfused (oxygenated), hypoxic (viable), and necrotic tumor regions.*

Materials and Methods: The experimental data for this study were acquired as described in detail previously[1]. The DCE-MRI signal intensity time-course data in the tumor region of interest (ROI) underwent pixel-by-pixel SSM pharmacokinetic analysis[7, 8]. The pre-contrast T_1 value was calculated by comparing the signal intensity of the DCE-MRI with that of the proton density MR images acquired before contrast agent injection. The arterial input function (AIF) curve shape was taken from a direct measurement in another DCE-MRI study[11] and temporally resampled to match the current DCE-MRI data. The AIF amplitude was then adjusted using a muscle ROI within the image field-of-view as reference tissue. To investigate the relationship of the SSM parameters K^{trans} and τ_i with the tumor microenvironment, masks selecting pixels in the tumor that are predominantly well perfused (P), hypoxic (H), or necrotic (N) were obtained by thresholding of *in vivo* Ak_{ep} maps (P), *ex vivo* pimonidazole (H) and Hematoxylin & Eosin (N) staining of tissue sections (**Fig. 1A**).

Results: The spatial, heterogeneous distribution of tumor perfusion/permeability (P), hypoxia (H) and necrosis (N) of a representative tumor slice from an experimental tumor (V = 1230 mm^3) are shown in **Fig. 1**. Qualitatively, K^{trans} (**Fig. 1B**) and Ak_{ep} (**Fig. 1A**) appear to be similarly spatially distributed and positively related, while high τ_i values (**Fig. 1B**) appear to correspond to tumor necrosis (N). Quantitatively (**Fig. 2**), perfused areas (P) are characterized by high Ak_{ep} (**Fig. 2A**) or high K^{trans} and low τ_i values (**Fig. 2B**), while necrotic areas (N) are characterized by low Ak_{ep} (**Fig. 2A**) or low K^{trans} and high τ_i values (**Fig. 2B**). Hypoxic areas (H) also have low Ak_{ep} or K^{trans}, and thus, cannot be separated from necrotic areas (N), using either parameter alone (**Fig. 2**). However, our preliminary data indicate that a combination of K^{trans} and τ_i can separate hypoxic from necrotic or perfused areas, as K^{trans} values are low and τ_i values cover an intermediate range in hypoxic areas (**Fig. 2B, histograms**).

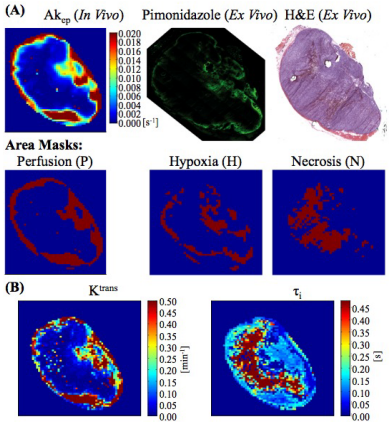

Figure 1: *(A) The top row shows an Ak_{ep} map and corresponding tissue sections depicting hypoxic and necrotic areas in a representative tumor slice (Adapted from[1]). The 2nd row displays the masks (obtained by 'thresholding') corresponding to perfused, hypoxic, and necrotic tumor areas. (B) K^{trans} and τ_i maps of the same tumor slice as in (A), obtained from the SSM analysis.*

Discussion / Conclusions: Our preliminary results indicate that a combination of K^{trans} and τ_i can separate areas that are predominantly viable/well-perfused or viable/hypoxic or necrotic. Overlapping values, as seen in the histograms distributions, are to be expected due to volume averaging, especially for pixels containing hypoxic cells located close to well-perfused areas[1]. These are indicative of pixels containing more than one tumor characteristic. For the purposes of predicting and monitoring cancer treatment response in the clinic, successful implementation of SSM analysis of DCE-MRI data may potentially obviate the need for additional imaging studies, such as ^{18}F-Fmiso PET, to assess the tumor microenvironment.

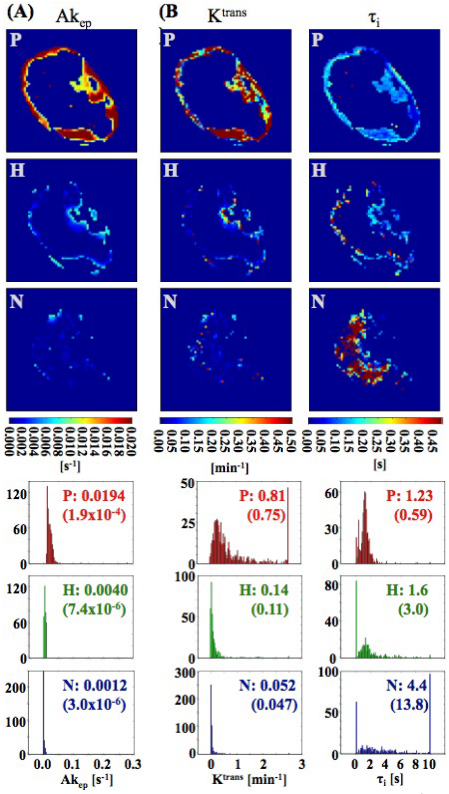

Figure 2: *Overlay of masks onto Ak_{ep} (A), K^{trans} and τ_i maps (B), depicting the spatial distribution of these parameters in well-perfused (P, top row), hypoxic (H, 2nd row), and necrotic (N, 3rd row) areas, while the bottom three rows display the corresponding histograms of the masked regions with mean (variance) denoted. Color scale as in Fig. 1.*

References: 1. Cho H *et al.* Neoplasia 2009. 11(3):247; 2. Vaupel P *et al.* Cancer Metastasis Rev 2007. 26(2):225; 3. Tatum JL *et al.* Int J Radiat Biol 2006. 82(10):699; 4. Vaupel P 2004. 14(3):198; 5. Ocak I *et al.* Front Biosci 2007. 12:3601; 6. Bhujwalla ZM *et al.* Topics Magn Reson Imaging 1999. 10(2):92; 7. Huang W *et al.* PNAS 2008. 105(46):17943; 8. Li X *et al.* Magn Reson Med 2005. 53(3):724; 9. Hoffmann U *et al.* Magn Reson Med 1995. 33(4):506; 10. Zhang Y *et al.* Biophys J 2011; 101:000; 11. Li X *et al.* J Magn Reson 2010. 206:190. **Acknowledgements:** Supported by NIH grants PO1 CA115675, R24 CA83084, NCI P30 CA0874, UO1 CA154602, and RO1 CA120861.